Макрогетероциклы
http://mhc-isuct.ru

DOI: 10.6060/mhc266997n

Activity Enhancement of Graphene Oxide/Zn Phthalocyanine Hybrid Photocatalysts in an Electric Field

Alsu G. Nugmanova,[a] Anna I. Gorshkova,[a,b] Dmitry A. Bunin,[a] Svetlana V. Monich,[a,c] Alexey E. Alexandrov,[a] Alexey A. Averin,[a] and Maria A. Kalinina[a@]

[a]*Frumkin Institute of Physical Chemistry and Electrochemistry, Russian Academy of Sciences, 119071 Moscow, Russia*
[b]*Department of Fundamental Physics-Chemical Engineering, Lomonosov Moscow State University, 119991 Moscow, Russia*
[c]*Chemistry Department, Lomonosov Moscow State University, 119991 Moscow, Russia*
[@]*Corresponding author E-mail: kalinina@phyche.ac.ru*

An optimized method has been developed for the synthesis of a hybrid photocatalyst GO/ZnPc based on octasodium salt of Zn(II) 2,3,9,10,16,17,23,24-octacarboxyphthalocyaninate (ZnPc*) and graphene oxide (GO). The hybrid assembly was achieved via non-covalent interaction through Zn(II) acetate ($Zn(OAc)_2$) to form a metal cluster, which prevents contact quenching of the chromophore's excited triplet state by the GO surface. The structure of the synthesized hybrid material was confirmed using fluorescence microscopy, Raman spectroscopy, and powder X-ray diffraction. The photocatalytic activity of the GO/ZnPc* hybrid was investigated in the model reaction of 1,5-dihydroxynaphthalene (DHN) decomposition under visible light irradiation. Additionally, the influence of a static external electric field (EEF) on the hybrid's efficiency was studied. The application of an EEF with a voltage of up to 4 kV allows for a 1.5-fold increase in the DHN decomposition reaction rate. The obtained data confirm the possibility of enhancing the photocatalytic activity of GO-based hybrid photocatalysts sensitized with various heterocyclic chromophores through exposure to an EEF.*

Keywords: Hybrid photocatalyst, zinc phthalocyaninates, graphene oxide, surface modification, photodegradation, photocatalysis, external electric field.

Усиление активности гибридных фотокатализаторов на основе оксида графена и фталоцианината цинка в электрическом поле

А. Г. Нугманова,[a] А. И. Горшкова,[a,b] Д. А. Бунин,[a] С. В. Монич,[a,c] А. Е. Александров,[a] А. А. Аверин,[a] М. А. Калинина[a@]

[a]*Институт физической химии и электрохимии им. А.Н. Фрумкина Российской академии наук, 119071 Москва, Россия*
[b]*Факультет фундаментальной физико-химической инженерии, Московский государственный университет им. М.В. Ломоносова, 119991 Москва, Россия*
[c]*Химический факультет, Московский государственный университет им. М.В. Ломоносова, 119991 Москва, Россия*
[@]*E-mail: kalinina@phyche.ac.ru*

Оптимизирован метод синтеза гибридного фотокатализатора ОГ/ZnPc на основе натриевой соли 2,3,9,10, 16,17,23,24-октакарбоксифталоцианината цинка (ZnPc*) и оксида графена (ОГ). Сборка гибрида производилась за счёт нековалентного взаимодействия через металлокластер – ацетат цинка(II) ($Zn(OAc)_2$), что предотвращает контактное тушение возбужденного триплетного состояния хромофора поверхностью ОГ. Структура гибридного материала подтверждена методами флуоресцентной микроскопии, КР-спектроскопии и порошковой рентгеновской дифракции. Фотокаталитическая активность гибрида ОГ/ZnPc* исследована в модельной реакции разложения 1,5-дигидроксинафталина (ДГН) под действием видимого света. Дополнительно изучено влияние статического внешнего электрического поля (ВЭП) на эффективность гиб-*

ридного фотокатализатора. Установлено, что применение ВЭП с напряжением до 4 кВ позволяет увеличить скорость реакции разложения ДГН в 1,5 раза. Полученные данные подтверждают возможность усиления фотокаталитической активности гибридных фотокатализаторов на основе ОГ, сенсибилизированных различными гетероциклическими хромофорами, за счёт воздействия ВЭП.

Ключевые слова: Гибридные фотокатализаторы, фталоцианинат цинка, оксид графена, модификация поверхности, фотодеградация, фотокатализ, внешнее электрическое поле.

Introduction

The chemical industry is fundamental to modern society and technological progress. However, conventional synthesis processes for essential products, ranging from pharmaceuticals and polymers to fuels, remain energy- and resource-intensive and are associated with the generation of persistent toxic pollutants.[1–3] In this context, technologies that align with the principles of green chemistry and sustainable development, based on the use of renewable energy, are becoming increasingly in demand.

Heterogeneous photocatalysis, which uses sunlight to drive chemical reactions for both synthesis processes and pollutant degradation, represents one of the most promising technologies.[4–8] Nevertheless, its extensive practical application is hindered by several limitations. These include the narrow spectral sensitivity of inorganic semiconductors (primarily in the UV region),[6–9] the rapid recombination of photoinduced charge carriers, as well as the low stability and selectivity of organic photosensitizers.[10]

One strategy to overcome these limitations is the development of hybrid materials that combine components with different photoactivation mechanisms[11,12] – charge transfer, characteristic of semiconductors,[9] and energy transfer, characteristic of molecular sensitizers.[13]

An additional synergistic effect can be achieved by modifying the photocatalytic process with external physical fields, such as ultrasonic, microwave, thermal, and others.[14] Currently, the application of an electric field is the most advanced, as it allows for the effective separation of photoinduced charges, suppressing their recombination.[15] At the same time, classical electrophotocatalysis, which requires immersing electrodes in the reaction medium, has serious drawbacks, such as the electrochemical degradation of components and high energy consumption.[15] A promising alternative is the use of an external electric field in a non-contact cell, but its efficiency critically depends on the dielectric response of the photocatalyst.

In this context, graphene oxide (GO) is of particular interest due to its incredibly high dielectric susceptibility ($\sim 10^6$).[16] This property opens the possibility for effectively controlling the spatial charge distribution in a hybrid photocatalyst under an external field.

It has been previously demonstrated that this approach can increase the reaction rate by a factor of 2.3 when sensitizing graphene oxide with porphyrin and perylene derivatives.[17] Despite the significant increase in reaction rate, the question of optimizing the sensitizer choice remains open: materials based on porphyrins are rather expensive and require complex synthetic procedures,[18,19] while perylene-based materials are considerably cheaper,[20] but the reaction rate, even when doubled, remains insufficient for industrial application.[17]

One promising solution to this problem is the use of more accessible and efficient sensitizers. In this context, phthalocyanine derivatives represent an optimal compromise between photoactivity, stability, and cost.[21–24] In the present work, octasodium salt of Zn(II) 2,3,9,10,16,17, 23,24-octacarboxyphthalocyaninate (ZnPc*) was chosen as the object of study, as it exhibits high photoactivity[24] in the visible region, comparable to that of porphyrins, while being more amenable to scaling.

This work is devoted to optimizing the composition of high-efficiency GO-based photocatalysts capable of enhanced activity under an external electric field (EEF). To this end, a hybrid material based on graphene oxide sensitized with a zinc phthalocyanine derivative (ZnPc*) was synthesized. Its photocatalytic activity was investigated in the model reaction of 1,5-dihydroxynaphthalene photodegradation, and a comparative assessment of the influence of an external electric field on the process kinetics was conducted.

Experimental

Materials and Methods

Water was preliminarily purified using a DE-10M water distiller and then deionized with a Vodolei deionizer. All reagents and solvents used during the synthesis and purification processes were of analytical grade and obtained from commercial sources (Merck, Sigma-Aldrich, Reakhim).

Weighing was carried out on an Ohaus AdventurerPro analytical balance.

Fluorescence microphotographs were taken with a confocal scanning microscope Horiba LabRAM HR Evolution (HORIBA Ltd., Kyoto, Japan) using a laser (532 nm, 50 mW). with a 50× objective.

Raman spectra were recorded with a Senterra system (Bruker) equipped with a 50× objective using excitation at a wavelength of 532 nm in the spectral range 1000–2000 cm^{-1}. All measurements were performed at an excitation laser power of less than 2 mW to avoid sample damage. The spectra were recorded for 100–500 s depending on a sample.

X-Ray diffraction (XRD) patterns were obtained using Empyrean (Panalytical) diffractometer equipped with 1-D position-sensitive X'Celerator detector. Ni-filtered Cu Kα-radiation was employed. Standard Bragg-Brentano (reflection) geometry was employed, allowing acquisition of out-of-plane diffraction.

^{1}H NMR spectra were recorded with a Bruker Avance III 600 spectrometer (600.13 MHz). Chemical shifts (d, ppm) were measured at T = 303 K.

UV–Vis spectra of solutions were recorded in 10 mm quartz cells by using spectrophotometer Jasco V-760.

Fluorescence spectra of solutions were recorded in 10 mm quartz cells by using spectrophotometer Jasco FP-8350.

The photocatalytic activity was evaluated in the reaction of 1,5-dihydroxynaphthalene (DHN) decomposition in an aqueous solution (10^{-4} M) under visible light irradiation (300 W xenon lamp equipped with AM1.5G and UVCut420 filters). For a typical test, 1 mg of the photocatalyst was dispersed in 2 mL of the DHN solution. Prior to illumination, the mixture was kept in the dark for 8 hours to establish adsorption-desorption equilibrium. Aliquots were collected every 10 minutes over a total irradiation time of 120 minutes. To study the influence of an electric field, a current source was used to apply a constant current of 0.2 mA and a voltage of 4 kV. The concentration of DHN in the solution was monitored spectrophotometrically by tracking the decrease in the intensity of the absorption band at $\lambda = 298$ nm.

Hydroxyl radical probing was performed in the water solution of terephthalic acid (TPA, 10^{-5} M). The excitation wavelengths of the solutions of TPA were 310 nm.

Synthesis

Octasodium salt of Zn(II) 2,3,9,10,16,17,23,24-octacarboxyphthalocyaninate (ZnPc).* A mixture of dimethyl 4,5-bis-(methoxycarbonyl)phthalonitrile (100 mg, 0.41 mmol, 1 eq.), zinc acetate (38 mg, 0.21 mmol, 0.5 eq.) and 1,8-diazabicyclo-[5.4.0]undec-7-ene (61 μL, 0.41 mmol, 1 eq.) in *n*-pentanol (5 mL) was degassed and refluxed under argon overnight. Then, *n*-pentanol was evaporated, and the dark-green sticky residue was sonicated with 50 vol. % aqueous EtOH, the precipitate was filtered, and washed with 50 vol. % aqueous ethanol. The dark-green solid was washed off the filter with chloroform. After solvent evaporation, this mixture of products was separated by column chromatography on silica through a gradient elution by a mixture of chloroform with hexane (30 → 0 vol. %), then with methanol (0 → 9 vol. %). Zinc(II) 2,3,9,10,16,17,23,24-octakis-(pentoxycarbonyl)phthalocyanine was eluted with a mixture containing 10 and 0 vol. % hexane, whereas some amounts of the hydrolyzed product were eluted with a mixture containing 1–5 vol. % methanol. These fractions were combined and refined by size-exclusion chromatography on Bio-Beads SX-1 (isocratic elution with a mixture of chloroform/methanol 97.5:2.5 v/v). The resulting product was mixed with a saturated aqueous sodium hydroxide solution (6 M, 6 mL), dry tetrahydrofuran (3 mL), and methanol (10 mL). The solution was degassed and then heated to 40 °C with vigorous stirring under argon for 1.5 h. The hydrolysis was monitored by thin-layer chromatography (TLC) [silica, hexane/acetone, 1:1 (v/v)]. During the hydrolysis reaction, the R_f of the reaction mixture decreased to zero providing evidence for the production of the sodium salt of the target compound. The reaction mixture was evaporated and washed with methanol to remove NaOH and other impurities, yielding the desired product ZnPc* as dark-blue powder. Yield: 28 mg, 32 %. ^{1}H NMR (600.13 MHz, D_2O): 9.63 (s, 8H, H_{Pc}).

Graphene oxide (GO) aqueous sols were synthesized from exfoliated carbon by a modified Hummers method.[25]

Hybrid photocatalyst ZnPc/GO* was synthesized by hydrothermal method. First, 3 mL of the GO hydrosol (10 mg/mL) was mixed with 7 mL of a $Zn(OAc)_2 \cdot 2H_2O$ solution ($5 \cdot 10^{-2}$ M) and treated in an ultrasonic bath for 30 minutes. Separately, 3 mg of ZnPc* was dissolved in 10 mL of water and also sonicated for 30 minutes. The resulting solutions were then combined and the final mixture was kept at 70 °C for 48 h to facilitate hybrid formation. The resulting suspension was filtered, washed with water, and lyophilized (–110 °C, 2 mPa, 4 h).

Results and Discussion

Synthesis and Characterization of the GO/ZnPc Hybrid*

A hybrid photocatalyst GO/ZnPc* was synthesized via a one-pot hydrothermal method. This approach facilitates the assembly of graphene oxide (GO) sheets with the zinc phthalocyanine derivative (ZnPc*) through non-covalent interactions mediated by zinc acetate. Critically, this coordination-based assembly strategy preserves the intrinsic high photoactivity of the ZnPc* chromophore. The zinc acetate linker creates a spatial separation that prevents direct π-stacking and suppresses contact quenching of the phthalocyanine's excited triplet state by the conductive GO surface, thereby maintaining efficient photophysical properties in the hybrid structure.[26]

The successful integration of the photoactive component into the GO matrix and the hybrid's structural features were confirmed by the complex of the physico-chemical methods. Fluorescence microscopy revealed distinct luminescent spots uniformly distributed across the material, providing direct visual evidence for the incorporation of the ZnPc* chromophores onto the GO surface (Figure 1a). To characterize the type of interactions in the hybrid material, Raman spectra were investigated for the initial GO (Figure 1b, *curve 1*); GO functionalized with zinc acetate (Figure 1b, *curve 2*); the initial chromophore, ZnPc* (Figure 1b, *curve 3*); and the GO/ZnPc hybrid (Figure 1b, *curve 4*). According to the data obtained, upon functionalization of GO with the zinc acetate metal cluster, a decrease in intensity and a shift of the D band, characteristic of GO, from 1350 cm^{-1} to 1380 cm^{-1} are observed. This confirms the formation of interactions via carboxyl groups between the metal cluster and graphene oxide (Figure 1b, *curves 1* and *2*). In the Raman spectrum of the final GO/ZnPc* hybrid, the positions and intensity ratio (I_D/I_G) of the characteristic D and G bands remain unchanged compared to GO functionalized with zinc acetate. Concurrently, new peaks appear at 687, 798, 1116, and 1518 cm^{-1} (Figure 1b, *curves 3* and *4*), which are the characteristic vibrational modes of the ZnPc* chromophore. These data confirm the formation of interactions through the metal cluster, without the formation of structures due to π–π stacking.

The crystallographic state of the hybrid was probed using powder X-ray diffraction (XRD). The XRD pattern of the freshly synthesized GO/ZnPc* (Figure 1c – *curve 2*) presents a number of peaks (at 4.5° and 9.0°) that do not correspond to the diffraction pattern of the free linker ZnPc* (Figure 1c – *curve 1*) at small angles (less than 15°), confirming the formation of crystalline phases in the hybrid GO/ZnPc*. The average size of the crystallites, calculated using the Scherrer equation,[27] was 16 nm for the hybrid GO/ZnPc*.

Photocatalytic Performance and Stability Assessment

The photocatalytic activity of the GO/ZnPc* hybrid was evaluated in the model reaction of 1,5-dihydroxynaphthalene (DHN) degradation under visible light irradiation. The catalyst demonstrated high initial activity, achieving significant DHN decomposition within the first 30 minutes

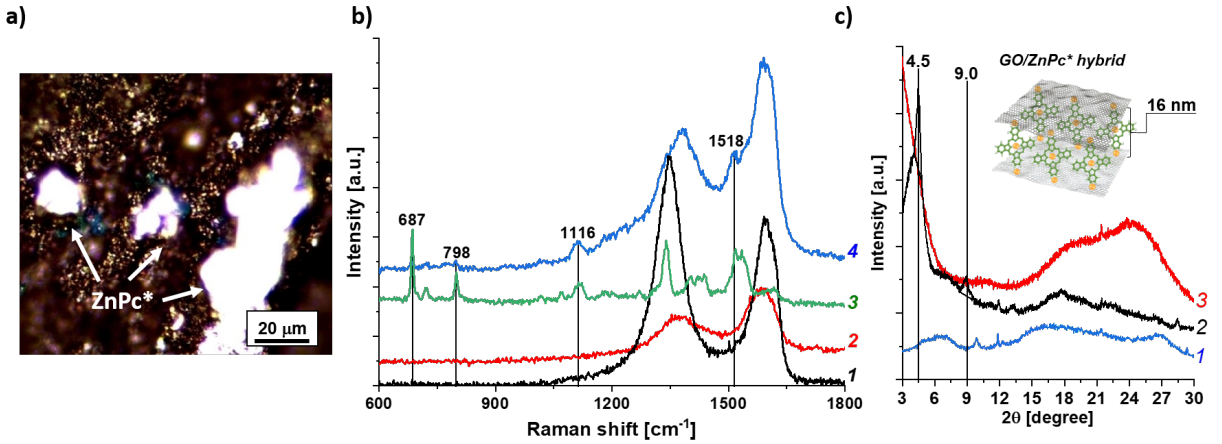

Figure 1. a) Fluorescence microphotograph of the GO/ZnPc*; b) Raman spectra: *curve 1* – GO, *2* – GO functionalized with $Zn(OAc)_2$, *3* – ZnPc* and *4* – hybrid GO/ZnPc*; c) XRD pattern of the ZnPc* – *curve 1*; hybrid GO/ZnPc*: *curve 2* – before, and *curve 3* – after photocatalytic reaction. Inset: modeled structures for GO/ZnPc*.

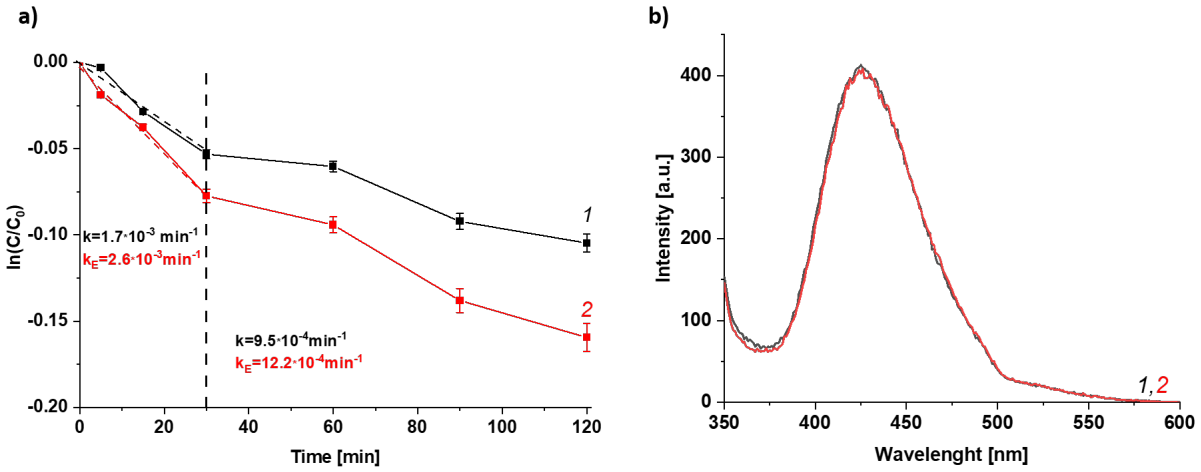

Figure 2. Kinetic curves of photocatalytic degradation DHN (10^{-4} M) in presence of GO/ZnPc*: 1 – without EEF, 2 – under EEF (4 kV); b) Fluorescent spectra of the TPA (10^{-5} M) after iiradiation in prescence GO/ZnPc*: 1 – without EEF, 2 – under EEF (4 kV).

of irradiation (Figure 2a). This initial rapid phase is attributed to the efficient generation of reactive oxygen species by photoexcited ZnPc*, facilitated by effective charge transfer to the GO matrix.

However, a pronounced decrease in the degradation rate was observed after this initial period. The reaction kinetics showed a marked slowdown, suggesting a loss of catalytic efficiency over time. This deactivation phenomenon was investigated by analyzing the catalyst post-reaction. Strikingly, the XRD pattern of the used GO/ZnPc* catalyst showed a complete disappearance of the crystalline peaks present in the fresh sample (Figure 1c, *curve 3*). This loss of long-range order suggests significant structural degradation of the hybrid, likely due to insufficient stabilization of the ZnPc* chromophore by the GO matrix. Under light, the chromophore undergoes photolysis, leading to the amorphization of the hybrid structure. The correlation between the kinetic slowdown and this loss of crystallinity confirms that the photodegradation of DHN competes with a parallel process of catalyst self-decomposition, ultimately limiting its long-term operational stability.

Enhancement by an External Electric Field (EEF)

To mitigate charge recombination and enhance performance, the influence of a static external electric field (EEF) on the photocatalytic process was investigated. Applying an EFF (4 kV) led to a measurable increase in the DHN degradation rate. Quantitative analysis of the kinetic data revealed a 1.5-fold enhancement in the reaction rate constant under the applied field compared to the standard photocatalytic conditions (Figure 2a).

This enhancement is ascribed to the efficient polarization of the GO component, which possesses an anomalously high dielectric susceptibility. The EEF promotes the spatial separation of photogenerated electron-hole pairs across the GO/ZnPc* interface. To gain deeper insight into the mechanism of field-induced enhancement, the generation of hydroxyl radicals (•OH) was monitored using a fluorescence probe assay with terephthalic acid (Figure 2b). Interestingly, the application of the EEF did not lead to a statistically significant increase in the •OH yield compared to the field-free experiment. This result suggests that the

enhancement of the overall photocatalytic activity is not primarily mediated through an accelerated formation of hydroxyl radicals.

Therefore, the primary mechanism of the activity boost is likely related to a more efficient utilization of the separated electrons. The applied field is proposed to facilitate the interfacial electron transfer from the conductive GO network to dissolved electron acceptors (*e.g.,* O_2), thereby increasing the rate of superoxide radical ($^{\bullet}O_2^-$) generation and suppressing the charge recombination pathway. This directed electron flux enhances the overall efficiency of the photocatalytic cycle without altering the fundamental pathway of $^{\bullet}OH$ generation. This result underscores the potential of non-contact electric field modulation as a viable strategy for boosting the efficiency of hybrid photocatalysts by steering specific charge transfer processes.

Conclusions

We have developed and studied a hybrid photocatalyst based on graphene oxide sensitized with a zinc phthalocyaninate derivative (GO/ZnPc*). This photocatalyst showed high initial activity in the photodegradation of DHN under visible light. Its efficiency can be increased by 1.5 times through the application of an external electric field in contactless cell, which enhances charge separation and interfacial electron transfer.

The key finding of this study is the identification of a critical stability issue: GO/ZnPc* undergoes significant structural degradation during operation, as confirmed by XRD. This degradation limits its long-term performance and practical application.

Thus, the main direction for future work is not merely performance enhancement but fundamental stabilization of the catalyst's architecture. Overcoming the stability barrier is essential for transitioning these promising hybrid materials from laboratory research to practical environmental applications.

Acknowledgements. The work was supported by the Russian Science Foundation (project no. 23-73-00095) and performed using the equipment of CKP FMI IPCE RAS.

Author contribution. A. Nugmanova: methodology, investigation, visualization, validation, writing – original draft; A. Gorshkova: resources, methodology, investigation, validation; D. Bunin: resources, methodology, validation, writing – review and editing; S. Monich: resources, methodology; A. Alexandrov: resources, methodology; A. Averin: resources, methodology, investigation; M. Kalinina: conceptualization, writing – review and editing, supervision, project administration, funding acquisition.

References

1. Anastas P.T., Bartlett L.B., Kirchhoff M.M., Williamson T.C. *Catalysis Today* **2000**, *55*, 11.
2. Hung Y.T., Turner B. Treatment of Wastewaters from Chemical Industries. In: *Integrated Natural Resources Research. Handbook of Environmental Engineering, Vol. 22* (Wang L.K., Wang M.H.S., Hung Y.T., Eds.) Springer, Cham, **2021**. pp. 69–102.
3. a) Singh P.K., Kumar U., Kumar I. et al. *Environ. Sci. Pollut. Res.* **2024**, *31*, 56428–56462; b) Medvedeva I.V., Medvedeva O.M., Studenok A.G., Studenok G.A., Tseytlin E.M. *ChemChemTech* **2023**, *66*(1), 6–27.
4. Ferreira M.E.C., Bergamasco R., Yamaguchi N.U. *J. Water Process Eng.* **2025**, *73*, 107734.
5. Ahmed S.N., Haider W. *Nanotechnology* **2018**, *29*, 342001.
6. Li H., Ye R., Zhou X. *Colloid J.* **2024**, *86*, 490.
7. Kumar A., Sharma P., Yadav D.D., Jha R. *Colloid J.* **2024**, *86*, 476.
8. Jagadeeswar V., Dhinesh V., Roopan S.M., Samuel E.J.J. *Colloid J.* **2023**, *85*, 827.
9. Opoku F., Govender K.K., van Sittert C.G.C.E., Govender P.P. *Adv. Sustainable Syst.* **2017**, *1*, 1700006.
10. Garland M.J., Cassidy C.M., Woolfson D., Donnelly R.F. *Future Medicinal Chemistry* **2009**, *1*, 667.
11. Di Y.M., Liu J.Y., Li M.H., Zhang S.Q., You M.H., Lin M.J. *Small* **2022**, *18*, 2201159.
12. Nugmanova A.G., Safonova E.A., Baranchikov A.E., Tameev A.R., Shkolin A.V., Mitrofanov A.A., Eliseev A.A., Meshkov I.N., Kalinina M.A. *Appl. Surf. Sci.* **2022**, *579*, 152080.
13. Romero N.A., Nicewicz D.A. *Chem. Rev.* **2016**, *116*, 10075–10166.
14. Hu C., Tu S., Tian N., Ma T., Zhang Y., Huang H. *Angew. Chem. Int. Ed.* **2021**, *60*, 16309.
15. Li J., Ren J., Li S., Li G., Li M.M.J., Li R., Kang Y.S., Zou X., Luo Y., Liu B., Zhao Y. *Green Energy Environ.* **2024**, *9*, 859.
16. Kumar K.S., Pittala S., Sanyadanam S., Paik P. *RSC Adv.* **2015**, *5*, 14768.
17. Nugmanova A.G., Sokolov M.R., Alexandrov A.E., Kniazeva M.A., Eremchev I.Y., Naumov A.V., Boukhvalov D.W., König B., Kalinina M.A. *J. Mater. Chem. A* **2025**, *13*, 200.
18. Senge M.O., Sergeeva N.N., Hale K.J. *Chem. Soc. Rev.* **2021**, *50*, 4730.
19. Hiroto S., Miyake Y., Shinokubo H. *Chem. Rev.* **2017**, *117*, 2910–3043
20. Giordano M., Cardano F., Barolo C., Viscardi G., Fin A. *Adv. Funct. Mater.* **2024**, *35*, 2411230.
21. Barker C.A., Zeng X., Bettington S., Batsanov A.S., Bryce M.R., Beeby A. *Chem. Eur. J.* **2007**, *13*, 6710.
22. Zvyagina A.I., Shiryaeva O.A., Afonyushkina E.Y., Kapitanova O.O., Averin A.A., Kormschikov I.D., Martynov A.G., Gorbunova Y.G., Veselova I.A., Kalinina M.A. *Small Methods* **2025**, *9*, 2401420.
23. Gregory P. *J. Porphyrins Phthalocyanines* **2000**, *4*, 432.
24. Marais E., Klein R., Antunes E., Nyokong T. *J. Mol. Catal. A: Chem.* **2007**, *261*, 36.
25. Sladkevich S., Gun J., Prikhodchenko P.V., Gutkin V., Mikhaylov A.A., Novotortsev V.M., Zhu J.X., Yang D., Hng H.H., Tay Y.Y., Tsakadze Z., Lev O. *Nanotechnol.* **2012**, *23*, 485601.
26. Nugmanova A.G., Gorshkova A.I., Yagodin A.V., Averin A.A., Kalinina M.A. *Colloid J.* **2023**, *85*, 961.
27. Fatimah S., Ragadhita R., Al Husaeni D.F., Nandiyanto A.B.D. *ASEAN J. Sci. Eng.* **2022**, *2*, 65.

Received 15.01.2026
Accepted 17.03.2026